



Diagnostic accuracy of an uncorrected native T1 mapping sequence for liver fibrosis and inflammation in autoimmune hepatitis: a prospective study using histopathology as reference standard

Natália B. N. Gomes^{1,2} · Ulysses S. Torres^{1,2} · Angela H. M. Caiado¹ · Patricia S. Fucuta³ · Maria Lucia C. G. Ferraz⁴ · Giuseppe D'Ippolito^{1,2}

Received: 1 May 2024 / Accepted: 25 July 2024
© Italian Society of Medical Radiology 2024

Abstract

Purpose There is an unmet clinical need for non-invasive imaging biomarkers that could replace liver biopsy in the management of patients with autoimmune hepatitis (AIH). In this study, we sought to evaluate the diagnostic accuracy of a simple uncorrected, non-contrast T1 mapping for detecting fibrosis and inflammation in AIH patients using histopathology as a reference standard.

Material and methods Over 3 years, 33 patients with AIH were prospectively studied using a multiparametric liver MRI protocol which included T1 mapping. Biopsies were performed up to 3 months before imaging, and a standardized histopathological score for fibrosis (F0–F4) and inflammatory activity (PPA0–4) was used as a reference. Statistical analysis included independent t test, Mann–Whitney U-test, and ROC (receiver operating characteristic) analysis.

Results T1 mapping values were significantly higher in patients with advanced fibrosis (F0–2 vs. F3–4; $p < 0.015$), significant fibrosis (F0–1 vs. F2–4; $p < 0.005$), and significant inflammatory activity (PPA 0–1 vs. PPA 2–4 $p = 0.048$). Moreover, the technique demonstrated a good diagnostic performance in detecting significant (AUC 0.856) and advanced fibrosis (AUC 0.835), as well as significant inflammatory activity (AUC 0.763).

Conclusion A rapid, simple, uncorrected, non-contrast T1 mapping sequence showed satisfactory diagnostic performance in comparison with histopathology for detecting significant tissue inflammation and fibrosis in AIH patients, being a potential non-invasive imaging biomarker for monitoring disease activity in such individuals.

Keywords Autoimmune hepatitis · Chronic hepatitis · Diagnostic imaging · Multiparametric magnetic resonance imaging

Abbreviations

AAR	Aspartate-to-alanine aminotransferase ratio
AIH	Autoimmune hepatitis
AILD	Autoimmune liver diseases
APRI	AST to platelet ratio index

ASC	Autoimmune sclerosing cholangitis
AUROC	Area under the receiver operating characteristic curve
cT1	Iron-corrected T1 relaxation maps
FIB-4	Fibrosis-4 index
FOV	Field of view
IAIHG	International autoimmune hepatitis group
MRE	Magnetic resonance elastography
MRI	Magnetic resonance imaging
MxSE	Highest sensitivity
MxSp	Highest specificity
PPA	Periportal/periseptal activity
PPV	Positive predictive value
ROC	Receiver operating characteristic curve
ROI	Region of interest
SD	Standard deviation
Se	Sensitivity
Sp	Specificity

✉ Natália B. N. Gomes
nataliaborgesnunes@gmail.com

¹ Grupo Fleury, São Paulo, Brazil

² Department of Diagnostic Imaging, Escola Paulista de Medicina, Universidade Federal de São Paulo (UNIFESP), Vila Clementino Rua Napoleão de Barros, 800, São Paulo, SP 04024-000, Brazil

³ Hospital de Base, Faculdade de Medicina de São José do Rio Preto (FAMERP), São Paulo, Brazil

⁴ Department of Gastroenterology, Escola Paulista de Medicina, Universidade Federal de São Paulo (UNIFESP), São Paulo, Brazil

TI	Inversion time
TE	Echo time
TR	Repetition time

Introduction

Autoimmune hepatitis (AIH) is an uncommon chronic liver disease with a high level of morbidity, accounting for up to 24% of liver transplants in the United States [1], and high mortality; approximately 40% of patients with severe untreated disease die within 6 months of diagnosis [2]. Invasive liver biopsy is typically recommended to stage and assess inflammation and fibrosis, inform treatment decisions in patients with inadequate response or clinical remission, and determine the possibility of withdrawing immunosuppression [3]. On the other hand, liver biopsy has the disadvantages of being invasive, costly, and not free of complications. It is particularly impractical for the long-term monitoring required in AIH [4], and, furthermore, it is subject to limitations such as sampling errors and high inter-observer variability [5].

As a result, there is currently an unmet clinical need for identifying non-invasive biomarkers that could effectively help in defining management strategies for AIH and reduce the frequency of liver biopsy [6]. Recent studies show that advanced magnetic resonance imaging (MRI) methods, such as T1 mapping, are promising for AIH [7], however, there is still a lack of prospective studies to validate and support these initial analyses. Studies on advanced liver MRI are specifically scarce in the field of AIH in comparison with other more frequent conditions (such as steatohepatitis), being also limited to small samples [8, 9] and, often, the absence of histological correlation utilizing biopsy, the current gold standard [6, 9]. Finally, they are hampered by the lack of simple, rapid, and widely available sequences not tied to commercial restrictions and patents [6, 10–13].

In search of more cost-effective alternatives with good reproducibility, recent studies have proposed MRI relaxometry with T1 mapping as an alternative method to assess liver fibrosis [14–16]. In addition, other emerging studies show that T1 mapping may be influenced by liver inflammation [17–19]. Unlike the Livermultiscan™ protocol's iron-corrected T1 map (cT1), still limited to the United States and some European countries [6, 10–13], the uncorrected, native (without contrast) T1 mapping technique does not require purchasing additional software and is easily configurable on any MRI machine, both 1.5 T and 3.0 T [20]. To our knowledge, no study has yet assessed the diagnostic performance of uncorrected native T1 mapping in staging liver fibrosis and inflammation using histopathology as the reference standard in AIH patients.

Therefore, the primary objective of this study was to prospectively evaluate the diagnostic value of a simple, uncorrected, native T1 mapping sequence in patients with AIH regarding liver fibrosis and inflammation, using histopathology as the gold standard.

Method

This was a prospective, observational, comparative, self-paired, non-randomized study. It followed Helsinki Declaration ethical guidelines and was approved by the Ethics Committee of the Federal University of São Paulo (approval number 97898718.6.3002.5474). All patients were required to sign a free and informed consent form.

Patients were sequentially recruited from the clinical hepatology unit of our institution, between October 2020 and April 2023. Given the rarity of the disease, we did not adopt a pre-established sample size goal calculated for statistical power, as this could substantially extend the study duration; however, we were careful that the sample was close to that of other similar reference studies in the field of AIH. Inclusion criteria encompassed patients with a confirmed diagnosis of AIH according to the simplified diagnostic criteria defined by the International Autoimmune Hepatitis Group (IAIHG) [21]. Patients had to agree to undergo blood sampling for laboratory analysis and multiparametric liver MRI up to a limit of 3 months after the liver biopsy as indicated by their clinical and therapeutic management. The exclusion criteria were as follows: (A) other autoimmune liver diseases (AILD), such as primary sclerosing cholangitis (PSC) and autoimmune sclerosing cholangitis (ASC); (B) overlap syndromes; (C) patients whose indication for biopsy has been suspended; (D) missing biopsy results or non-diagnostic image quality; (E) patients who did not agree or had contraindications to the MRI procedure (Fig. 1).

Histopathological analysis

Biopsies were performed using ultrasound orientation/guidance using the Tru-Cut technique with an automated 14G diameter needle, which allowed sampling from the right hepatic lobe. Specimens were fixed in formalin and embedded in paraffin. Only specimens with more than 10 mm in length and more than six intact portal tracts were considered for analysis [22]. Due to the substantial inter-observer variation in liver biopsy analysis [5], the specimens' histopathological analysis was performed only before MRI by one experienced liver pathologist of our institution (with 20 years of experience in liver biopsy analysis), blinded to all other clinical data (including MRI).

For fibrosis staging, the Metavir score [23] was used: F0—absence of fibrosis; F1—periportal fibrosis; F2—periportal

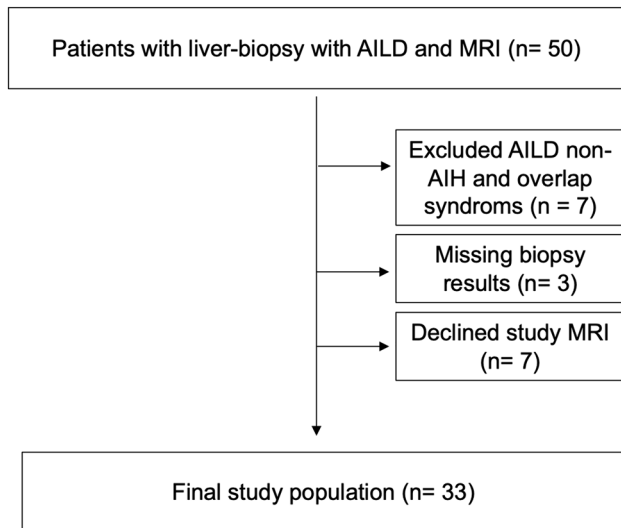


Fig. 1 Flowchart of patients inclusion. AILD, autoimmune liver diseases; AIH, autoimmune hepatitis; MRI, magnetic resonance imaging

fibrosis with few bridges or septa; F3—bridging fibrosis; F4—cirrhosis. Patients F2–4 were classified as significant fibrosis, and those F3–4 as advanced fibrosis [24].

The Desmet classification with a scoring scale from 0 to 4 was used to grade the histologic inflammation [25], according to periportal/periseptal activity (PPA). Patients were divided into 2 groups: PPA0–1 vs. PPA2–4 as resolved or low histologic inflammation and active histologic inflammation, respectively. This grouping was based on histologic information relevant to clinical decision-making regarding the maintenance or discontinuation of immunosuppressive therapy [26].

MRI technique

The examinations were performed up to three months after the biopsy, with a 1.5 T equipment (Magnetom Aera 1.5 T, Siemens Healthcare, Erlangen, Germany). T1 and T2 weighted sequences, diffusion, hydrogen proton spectroscopy, proton density, T1 mapping, and fat fraction sequences were performed, as well as an R2* sequence using a standardized fat- and noise-corrected R2* fitting algorithm on the vendor's native multi-echo gradient-echo sequence, as previous studies demonstrate consistent and highly reproducible linear R2*-LIC calibration at both 1.5 T and 3.0 T, independent of scanner vendor [27].

T1 mapping was obtained in 1 min and 20 s using the sequence modified look-locker inversion recovery (MOLLI), acquired in breath-hold with no respiratory and/or cardiac gating. The scan duration/breath-hold was 14.0 s. Three liver slices were acquired for the T1 map sequence with the center

at the level of the liver hilum in order to cover as much liver parenchyma as possible, without the administration of contrast medium, with the following parameters: TR (repetition time) /TE (echo time)=2.5/1.06 ms; flip angle, 35°; number of excitations, 1.0; field of view (FOV), 340×273 mm; matrix, 192×124; acceleration factor, 2; nonselective inversion pulse; steady-state free precession single-shot readout sequence; fixed time interval TR, 700 ms; minimum inversion time (TI), 100 ms; slice thickness, 8 mm; inversions number, 3; number of findings after inversion pulse, 3, 3, 5; number of recoveries after each inversion pulse, 4, 4, 0; TI increment between inversions, 80 ms, according to a protocol already published in the literature [28]. It is noteworthy to mention that with the technical data of this sequence, any MRI equipment programmer can configure the T1 map sequence without the need of purchasing any additional software package.

Image analysis

All MRI studies were interpreted in consensus by two abdominal radiologists (NBNG, 5 years of experience, UST, 10 years of experience) blinded to patient clinical and demographic data. For liver T1 measurements, parametric maps were generated for each anatomical slice. As there is substantial heterogeneity and no clearly established method across the studies in the literature to quantify T1 relaxation time from the liver T1 map, different regions of interest (ROI) were obtained for T1 mapping, aiming at being as comprehensive and exhaustive as possible in the exploration of the various measurement methods to establish the most feasible one, as detailed below:

- T1 map (circled ROI RL 1 slice): One ROI in the right hepatic lobe (RL) in one single slice of the liver, placed in the liver VIII segment, from where most percutaneous biopsies are taken, approximately midway between the hepatic portal and the hepatic surface, avoiding bile and vascular structures (Fig. 2A) [29].
- T1 map (mean 3 circled ROI 1 slice): Three circled ROIs in one single slice of the liver, including the RL and left medial section, excluding dilated biliary and visible vascular structures (Fig. 2B) [30].
- T1 map (whole liver 1 slice): The ROI was drawn to cover the largest possible area of liver parenchyma without including large blood vessels and bile ducts. While placing the ROI, a distance from the organ capsule of at least 1 cm was maintained (Fig. 2C) [31].
- T1 map (whole liver 3 slices): The ROIs were drawn to cover the largest possible area of liver parenchyma, one per anatomical level. Then an average of the three ROIs was obtained (Fig. 2C–E) [30].

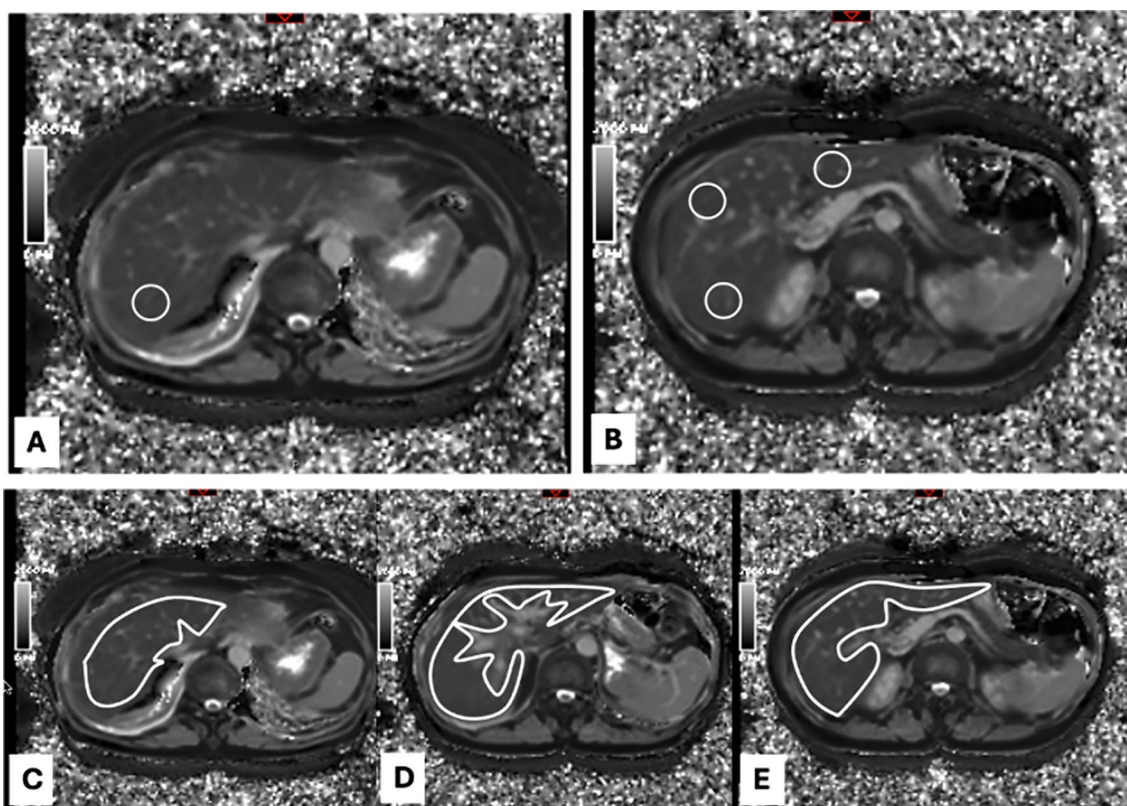


Fig. 2 Representative cases of different ROIs obtained to measure T1 relaxation using the T1 mapping sequence. **A.** One circled ROI in a single slice of the liver. **B.** Three circled ROIs in a single slice. **C.**

One free-hand ROI that includes the entire liver in a single image. **C–E.** Three free-hand ROI's including the entire liver in three slices

PDFF and $R2^*$ values were obtained applying a $3 \times 3 \times 3$ cm voxel on the segment VI–VII, avoiding artifacts, blood vessels of larger caliber and bile ducts [32]. The PDFF fraction was calculated based on the Longo et al. standard formula [32, 33]. A large ROI was drawn through the mid right lobe on a single image to measure proton density fat fraction and iron concentration, avoiding visible blood vessels and dilated bile ducts [32, 34]. The classification adopted for the grading of the fat fraction by the PDFF method and the spectroscopic method was as follows [35]: Grade 0 (Normal) < 5%; Grade I (Mild) > 5–15%; Grade II (Moderate) > 15–25%; and Grade III (Severe) > 25%. $R2^*$ was used to estimate liver iron concentration (LIC). The following classification was used: Absent < 2 mg/g; Insignificant 2–4 mg/g; Mild > 4–6 mg/g; Moderate > 6–8 mg/g; Moderate to severe > 8–16 mg/g; and severe > 16 mg/g [36].

Statistical analysis

The descriptive analysis included absolute and relative frequencies for categorical variables and mean, median,

standard deviation, and variation for continuous variables. The normal distribution of continuous variables was analyzed by asymmetry, kurtosis, and Shapiro–Wilk test. Student's t-test or Mann–Whitney test were used for the comparison of continuous variables. Associations between categorical variables were tested using Fisher's exact test. The accuracy of laboratory and MRI variables in predicting significant fibrosis, advanced fibrosis, and periportal/periseptal inflammatory activity was determined by the measurement of the area under the ROC curve (AUROC), and the comparative analysis between them was performed using the DeLong test. The best cutoffs to predict the outcomes were determined by the Youden index. Diagnostic accuracy was also evaluated by the calculation of sensitivity, specificity, positive predictive value, and negative predictive value. With the aim of verifying cutoff points for different contexts, prioritizing sensitivity or specificity, four more methods were applied in addition to the Youden method to find the appropriate cutoff points for these different situations. All tests were two-tailed and values of $p < 0.05$ were considered significant. The statistical analysis was performed using the IBM-SPSS Statistics software version 29.

Results

Descriptive analysis

Most patients in the study were female, 29/33 (87.9%), with a mean age of 46 years. The baseline characteristics of the studied sample are detailed in Table 1. Regarding non-invasive fibrosis markers, the median values for APRI (AST to Platelet Ratio Index) and FIB-4 (Fibrosis-4 Index) were 1.20 (range 0.10–21.40) and 2.30 (range 0.33–14.94), respectively.

In the biopsy studies, it was not possible to analyze the periportal/periseptal activity in the fragments obtained in 1 patient. Histopathologic analysis diagnosed 4 patients with F0 (12.1%), 6 with F1 (18.2%), 9 with F2 (27.3%), 12 with F3 (36.4%) and 2 with F4 (6.1%). One-third (10/33 30.3%) were classified as non-significant fibrosis (F0–1) and almost two-thirds (19/33 57.6%) as non-advanced fibrosis (F0–2)

Table 1 Baseline characteristics of the studied sample

Variable	N=33
Age, years	46.2 ± 14.3
Gender, n (%)	
Female	29 (87.9)
Male	4 (12.1)
Laboratory tests	
Hb (g/dL)	13.53 ± 1.2
Ht (%)	40.17 ± 3.6
Leucocytes (per microliter)	7,117.42 ± 3,864.5
Neutrophils (per microliter)	4,136.81 ± 2,455.4
Lymphocytes (per microliter)	1,965.84 ± 1,140.9
Neutrophil / Lymphocyte	5.51 ± 19.1
Platelets (per microliter)	221,687.5 ± 99,198.2
AST (xULN)	6.19 ± 8.2
ALT (xULN)	5.76 ± 7.4
ALT/AST	0.97 ± 0.6
ALP (xULN)	1.63 ± 1.7
GGT (xULN)	5.59 ± 6.8
INR	1.10 ± 0.1
Albumine (g/dL)	3.94 ± 0.4
Total bilirubin (mg/dL)	2.63 ± 4.2
Direct bilirubin (mg/dL)	1.88 ± 3.4
Indirect bilirubin (mg/dL)	0.72 ± 1.0
Immunoglobulin M (IU/mL)	230.12 ± 381.1
Immunoglobulin G (IU/mL)	2015.84 ± 970.3

Continuous variables are described as mean ± standard deviation; categorical variables are described in number (percentage)

Hb, hemoglobin; Ht, hematocrit, AST, aspartate aminotransferase; ULN, Upper normal limit; ALT, alanine aminotransferase; ALP, alkaline phosphatase; GGT, gamma glutamyltransferase; INR, international normalize

(Table 2). Regarding inflammatory activity, we identified 4 patients with score 0 (12.5%), 2 with score 1 (6.3%), 10 with score 2 (31.3%), 12 with score 3 (37.5%) and 4 with score 4 (12.5%), accounting for 6/32 (18.8%) as low or absent inflammatory activity (PPA 0–1) and 26/32 (81.2%) as higher inflammatory activity (PPA 2–4) (Table 2).

Seven patients had hepatic steatosis (7/33 21.2%), all of them with a discrete degree (liver fat fraction between 5 and 15%). None of the patients in the study showed iron accumulation according to the MRI R2* method. The mean and standard deviation values of PDFF were 2.74 and 3.60, and of R2* were 23.52 and 4.57, respectively. T1 map was analyzed by steatosis and iron accumulation groups, but data were insufficient to calculate significance.

Comparative analysis

Advanced fibrosis

The four techniques used to measure the derived values from the T1 mapping demonstrated statistically higher values in advanced fibrosis compared to non-advanced fibrosis ($p < 0.015$) (Table 3, Fig. 3). The highest accuracy in the discrimination of advanced fibrosis from non-advanced fibrosis groups was observed for the T1 map whole liver 1 slice (AUC 0.835) and whole liver 3 slices (AUC 0.801), considering a cutoff of 689 ms and 683.3 ms, respectively (Table 4, Fig. 4).

Significant fibrosis

Mean T1 values were significantly higher in patients with significant fibrosis (F2–4) compared to those with no or mild fibrosis (F0–1) using all four techniques derived from T1 mapping ($p < 0.05$) (Table 3).

ROC analysis showed good diagnostic performance of T1 mapping to discriminate significant fibrosis using the four different T1 measurement techniques, all with AUC > 0.800 (Table 4). The highest accuracy in distinguishing significant vs. non-significant fibrosis groups was achieved using T1 map whole liver 1 slice (AUC 0.857) and whole liver 3 slices (AUC 0.857), using a cutoff of 689 ms and 617 ms, respectively (Table 4).

Inflammatory activity

Among the T1 map variables, only the whole liver one slice's technique showed a significant difference in the PPA 2–4 group ($p = 0.048$), ranging from 631.5 (549.0–651.0) in the absence or low inflammation (PPA 0–1) to 687.5 (578.0–870.0) in the group with more inflammatory activity (Table 3, Fig. 5 and 6). The AUC to discriminate

Table 2 Descriptive analysis of histological data

Variable	Frequency (%)
Fibrosis score	
0	4/33 (12.1)
1	6/33 (18.2)
2	9/33 (27.3)
3	12/33 (36.4)
4	2/33 (6.0)
Significant fibrosis	
Non-significant fibrosis (F0–F1)	10/33 (30.3)
Significant fibrosis (F2–F4)	23/33 (69.7)
Advanced fibrosis	
Non-advanced fibrosis (F0–F2)	19/33 (57.6)
Advanced fibrosis (F3–F4)	14/33 (42.4)
Periportal/periseptal activity (PPA)	
0	4/32 (12.5)
1	2/32 (6.3)
2	10/32 (31.3)
3	12/32 (37.5)
4	4/32 (12.5)
Periportal/periseptal activity	
PPA 0–1	6/32 (18.8)
PPA 2–4	26/32 (81.2)

PPA, Periportal / periseptal activity

the inflammatory activity group was 0.763 (Table 4), considering a cutoff of 654 ms.

Cutoff points

The cutoff points with the highest sensitivity (MxSE) and NPV for T1 map whole liver 1 slice were 618.00 ms for advanced fibrosis, 592.00 ms for significant fibrosis and 578.00 ms for inflammatory activity.

On the other hand, the cutoff points with the highest specificity (MxSP) and PPV for T1 map whole liver 1 slice were 806.00 ms for advanced fibrosis, 689.00 ms for significant fibrosis and 654.00 ms for inflammatory activity.

Discussion

This study reports the diagnostic performance of native T1 maps to differentiate significant fibrosis, advanced fibrosis, and advanced inflammation in patients with autoimmune hepatitis- contributing to answer an important question in the literature concerning uncorrected native T1 mapping: is iron correction really necessary? Previous studies have hinted to the fact that patient groups with low iron concentration can be differentiated and followed-up using native T1 mapping, but prospective evidence, such as presented in this manuscript was lacking. Having

studied a fairly significant number of case of a relatively rare disease (such as AIH), we have demonstrated that an uncorrected, native (i.e., non-contrasted) T1 mapping sequence has good accuracy in detecting significant liver fibrosis and inflammation in patients with AIH when using histopathological analysis from biopsy specimens as the reference standard; this was also the first study to test several techniques for T1 measurement, showing that a rapid and easy-to-perform whole liver 1-slice technique for measurement emerged as that showing the best diagnostic performance in discriminating the significant (AUC 0.856) and advanced fibrosis groups (AUC 0.835), as well as inflammatory activity group (AUC 0.763), with potential impact and usage in clinical routine.

In our analyses, we grouped the patients according to the degree of inflammation and the fibrosis stages. Hepatic fibrosis is often preceded by chronic inflammation, and persisting inflammation has been associated with progressive hepatic fibrosis and developing cirrhosis [37]. Classification of patients by fibrosis stage is important because it has prognostic significance. Significant fibrosis identifies patients with potentially progressive disease [37]. Advanced stages of fibrosis are associated with negative endpoints such as decompensated cirrhosis and/or hepatocellular carcinoma [37]. Moreover, patients were divided into two inflammatory groups (having resolved or low histologic inflammation versus active histologic inflammation); this classification

Table 3 Comparative analysis of T1 map measurement techniques in predicting fibrosis categories and inflammatory activity

Liver fibrosis						
T1 map	Non-advanced fibrosis (F0–F2)		Advanced fibrosis (F3–F4)		P value	
	N	Median (min–max)	N	Median (min–max)		
T1 map (circled ROI RL 1 slice)	19	594.0 (521.0–1,082.0)	14	685.0 (563.0–1,184.0)	0.015*	
T1 map (mean 3 circled ROI 1 slice)	18	605.4 (499.7–792.0)	14	683.0 (572.7–944.3)	0.010*	
T1 map (whole liver 1 slice)	19	640.0 (549.0–777.0)	14	721.0 (618.0–870.0)	0.001*	
T1 map (whole liver 3 slices)	19	631.3 (542.0–769.7)	14	700.2 (620.3–873.0)	0.004*	
	Non-significant fibrosis (F0–F1)		Significant fibrosis (F2–F4)			
T1 map (circled ROI 10 RL 1 slice)	561	(521–736) 23		671 (532–1,184)	0.005*	
T1 map (mean 3 circled ROI 1 slice)	9	578.3 (499.7–667) 23		662.7 (572.7–944.3)	0.003*	
T1 map (whole liver 1 slice)	10	591 (549–686) 23		710 (592–870)	0.001*	
T1 map (whole liver 3 slices)	10	608.6 (542–698.2) 23		687.3 (617–873)	0.001*	
	Inflammatory activity					
		PPA (0–1)		PPA (2–4)		
T1 map (circled ROI RL 1 slice)	6	625.0 (521.0–810.0)	26	658.5 (536.0–1,184.0)	0.359*	
T1 map (mean 3 circled ROI 1 slice)	6	605.35 (499.7–640.7)	25	662.7 (540.7–944.3)	0.110*	
T1 map (whole liver 1 slice)	6	631.5 (549.0–651.0)	26	687.5 (578.0–870.0)	0.048*	
T1 map (whole liver 3 slices)	6	644.8 (542.0–676.0)	26	687.65 (586.6–873.0)	0.134*	

Continuous variables are represented as median (minimum; maximum) or mean ± standard deviation

* Mann–Whitney test

PPA, Periportal / periseptal activity; ROI, Region of interest; RL, Right lobe

was based on histologic information that was important for clinical decision-making regarding the maintenance or discontinuation of immunosuppressive drugs [37].

In recent years, there have been significant advances in non-invasive MR imaging for the detection of hepatic

fibrosis, and T1 maps have shown promising results in differentiating noncirrhotic from cirrhotic patients in different Child–Pugh stages [28, 38], and in estimating liver function in both 1.5 T and 3 T MR equipment [38]. Recently, T1 mapping was even shown to be able to stage

Fig. 3 A 65-year-old woman with advanced fibrosis (F3) due to AIH. On the left, the T1 map shows the T1 relaxation time value of 823 ms. Histologic specimen from liver biopsy is shown on the right. Reticulin staining showing portal spaces widened by fibrosis with portal-portal and portal-centered septa emanating and forming nodules

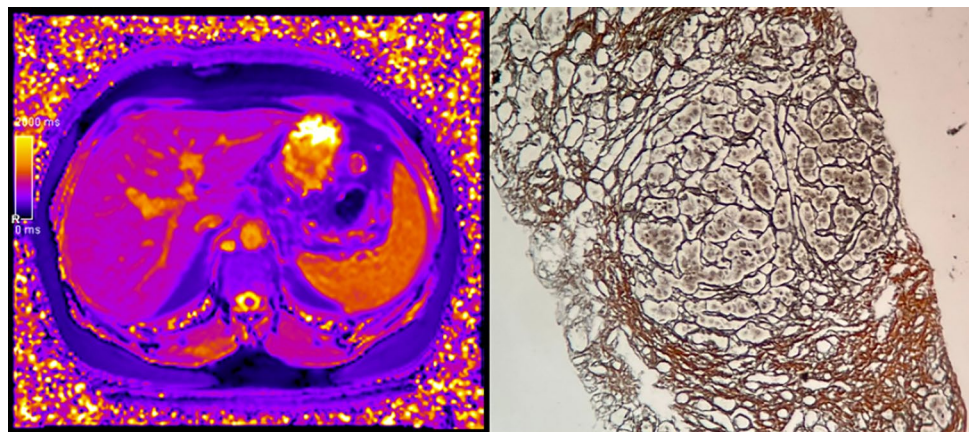


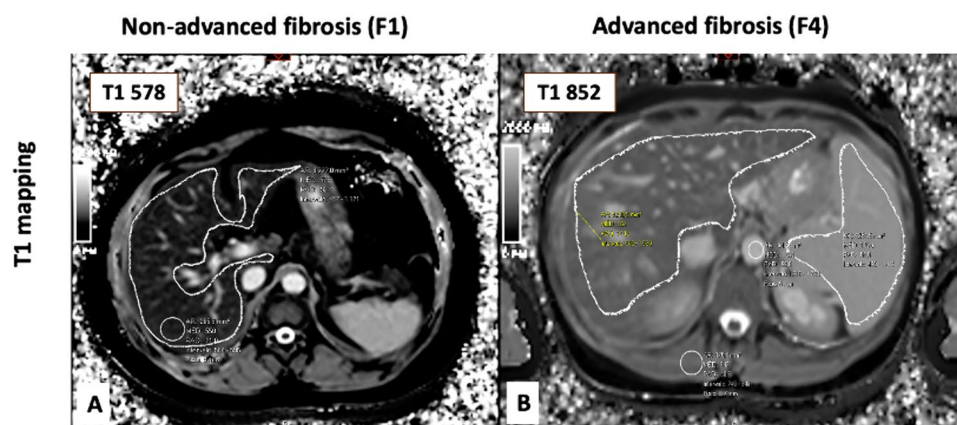
Table 4 Performance of T1 map measurement techniques in predicting fibrosis categories and inflammatory activity

	Cutoff*	AUC	CI 95% LL	CI 95% UP	Se	Sp	PPV	NPV
<i>Advanced fibrosis (F0–2 × F3–4)</i>								
T1 map (circled ROI RL 1 slice)	638	0.752	0.585	0.919	0.786	0.632	0.611	0.800
T1 map (mean 3 circled ROI 1 slice)	662.7	0.770	0.604	0.936	0.643	0.778	0.692	0.737
T1 map (whole liver 1 slice)	689	0.835	0.696	0.973	0.714	0.842	0.769	0.800
T1 map (whole liver 3 slices)	683.3	0.801	0.650	0.951	0.786	0.737	0.687	0.824
<i>Significant Fibrosis (F 0–1 × F 2–4)</i>								
T1 map (circled ROI RL 1 slice)	563	0.809	0.637	0.980	0.957	0.600	0.846	0.857
T1 map (mean 3 circled ROI 1 slice)	584	0.845	0.691	1.000	0.913	0.667	0.875	0.750
T1 map (whole liver 1 slice)	689	0.857	0.719	0.994	0.565	1.000	1.000	0.500
T1 map (whole liver 3 slices)	617	0.857	0.697	1.000	1.000	0.700	0.885	1.000
<i>Inflammatory Activity (PPA 0–1 × PPA 2–4)</i>								
T1 map (circled ROI RL 1 slice)	536	0.622	0.333	0.910	1.000	0.333	0.867	1.000
T1 map (mean 3 circled ROI 1 slice)	660.7	0.713	0.523	0.904	0.560	1.000	1.000	0.353
T1 map (whole liver 1 slice)	654	0.763	0.589	0.936	0.654	1.000	1.000	0.400
T1 map (whole liver 3 slices)	683.3	0.699	0.505	0.892	0.615	1.000	1.000	0.375

* cutoff by Youden Index

F, staging of fibrosis (liver biopsy); PPA, periportal/periseptal activity (liver biopsy); AUC, area under the ROC curve; CI, confidence interval; LL, lower limit; UP, upper limit; Se, sensitivity; Sp, specificity; PPV, positive predictive value; NPV, negative predictive value; ROI, region of interest

Fig. 4 Representative liver T1map images of patients with (A) non-advanced fibrosis (F1-T1: 578 ms) vs. (B) advanced fibrosis (F4-T1: 851 ms), showing higher values as fibrosis progresses. F, fibrosis stage



liver fibrosis in a sample with a mix of liver diseases [19]. The diagnostic performance of the uncorrected T1 map sequence was assessed once in autoimmune hepatitis for the identification of significant fibrosis (AUC: 0.846), which was similar compared to clinical fibrosis scores [APRI, FIB-4, and aspartate-to-alanine aminotransferase ratio (AAR)], using MRE (magnetic resonance elastography) as a reference standard [9]. However, there are no studies using T1 mapping with histopathology as a reference standard in staging liver fibrosis and inflammation in a specific AIH setting.

Regarding the assessment of hepatic inflammation using uncorrected T1 mapping, von Ulmenstein et al. [19] showed that T1 values were significantly higher in patients with

inflammation (A0 vs. A1–2, both $p=0.01$), with an AUC of 0.72 [19]. The mixed population of patients with different liver diseases and different classifications of inflammatory activity and fibrosis, however, which were unified for statistical analysis, are important limitations of this study.

It should be pointed out that T1 relaxation time increases in parallel with an increase in extracellular fluid volume, which is characteristic of fibrosis and inflammation [39]. In addition, because T1 mapping is a non-invasive composite biomarker of fibro-inflammation, it cannot currently measure one independently of the other [12]. Thus, although high values on T1 mapping do not imply the presence of both fibrosis and inflammation simultaneously, future work is underway to improve the

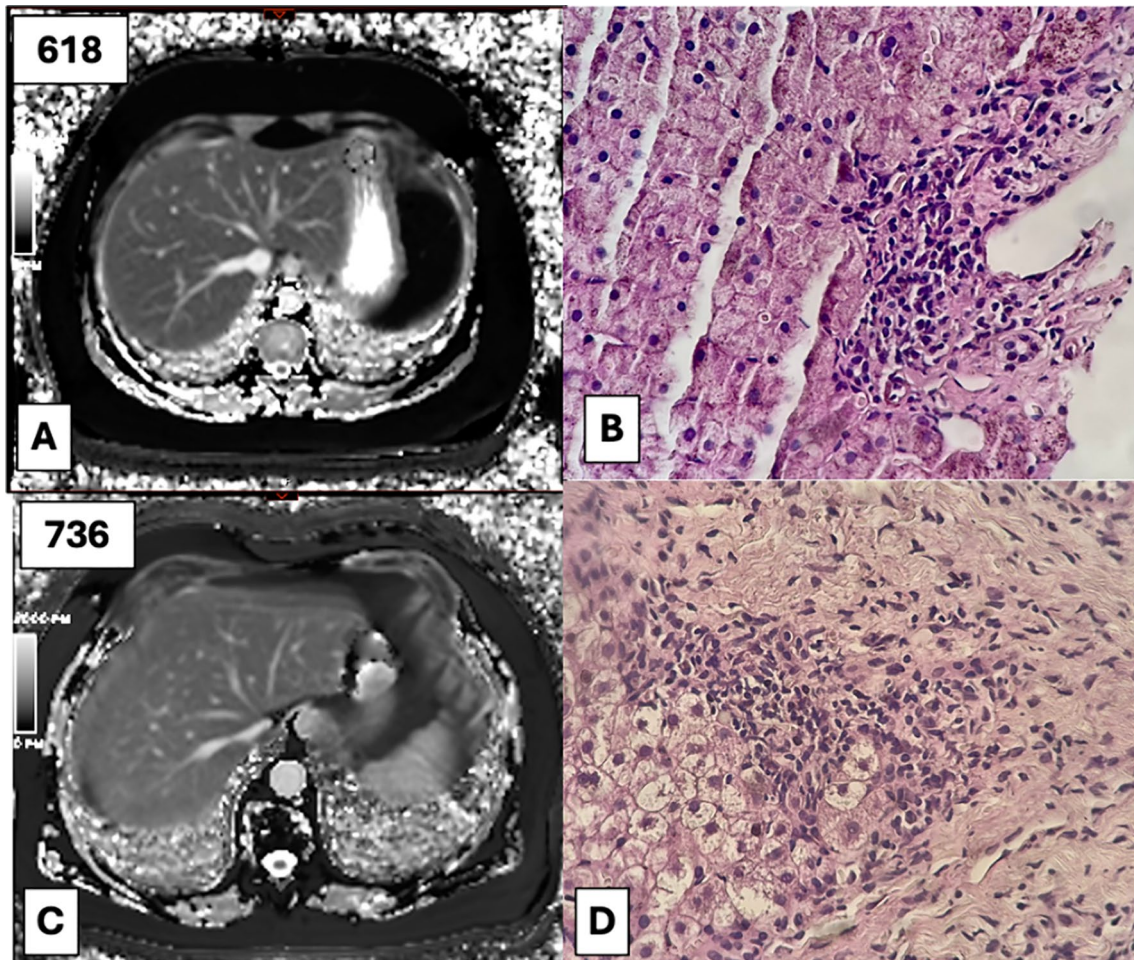
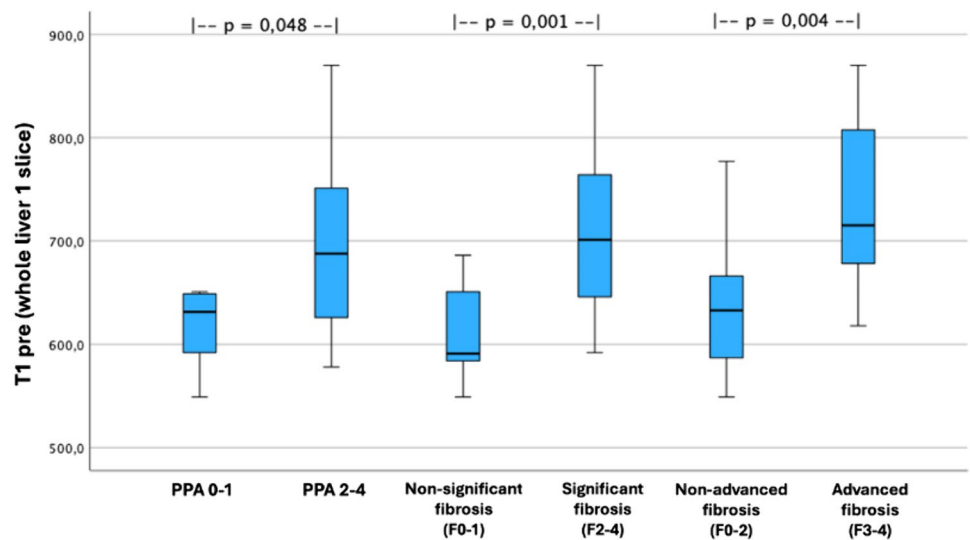


Fig. 5 Two representative cases of different T1 map patterns in hepatic inflammatory activity. Above, a patient with low inflammatory activity (PPA 1—images **A** and **B**). T1 relaxation time was 618 ms. Below, a patient with more inflammatory activity (PPA 3—images **C** and **D**). We observed higher T1 relaxation values

of 736 ms. Figures **B** and **D** illustrate the histologic inflammatory activity. Figure **B** shows the lack of periportal/periseptal activity. Figure **D** shows a lymphomonuclear infiltrate with plasma cells and interface hepatitis

Fig. 6 Boxplot graphs for T1 mapping (whole liver 1 slice) in the bivariate comparative analyses, in relation to histologic inflammation and fibrosis. It is possible to verify that there is a significant difference in the T1 map values to discriminate between PPA 0–1 × PPA 2–4; F0–1 × F2–4; and F0–2 × F3–4



biomarker so that it can distinguish between fibrosis and inflammation [12]. However, although we obtained satisfactory and statistically significant values when analyzing such variables separately, we were not able to distinguish fibrosis from liver inflammation based on T1 maps. This highlights the need to further evaluate the performance of the uncorrected T1 map in a larger cohort to validate its utility in a generalized clinical setting.

Another advanced MRI sequence derived from the T1 map that has recently been the subject of much research is the corrected T1 map. Corrected T1 mapping of the liver is a commercially available method for quantifying T1 relaxation, adjusted for the T2* effect, MR system manufacturer, and field strength [29]. Although there are still few studies on cT1 in AIH, excellent results have been found. However, these were limited to the pediatric population and young adults. Associations between cT1 and histology in pediatric patients showed a significant positive correlation between cT1 and Kleiner Brunt's fibrosis ($r=0.38$, $P=0.001$) in 58 patients with AIH [12] and Metavir fibrosis score ($r=0.41$, $P=0.02$) [40] in 35 AILD cases. Despite the excellent results in the fibro-inflammatory assessment of the liver in AIH at baseline and follow-up, the iron-corrected T1 relaxation maps (cT1) [6, 10–12] are not yet available from major equipment manufacturers, commercially offered only as post-processing software (LiverMultiScan™, Diagnostics, Oxford, UK), making it less accessible, currently concentrated in the US and few centers in Europe [41].

To date, few studies have addressed the relationship between T1 mapping and histologic inflammation in AIH, all limited to cT1 in a specific sample of children and adolescents [11, 12, 40], most including ASC patients [11, 40]. Positive correlations were found between cT1 and portal ($r=0.35$ – 0.41 , $p<0.001$) and lobular inflammation ($r=0.31$ – 0.32 , $p<0.016$) in AILD [11, 12]. Recently, in 2023, Trout et al. showed a higher correlation of cT1 values with histologic inflammation ($r=0.60$ $p<0.001$). In addition, the diagnostic performance of cT1 for discriminating histologic inflammation was evaluated for the first time, with good results. The AUC for discriminating HAI scores of 0–3 from scores greater than 3 was 0.87 (95% CI, 0.74–0.99) for cT1 [40]. Although we did not compare the uncorrected T1 map with the corrected T1 map, the results obtained in our study are similar to those recorded in studies that adopted the cT1 map to differentiate the degrees of fibrosis and inflammation, suggesting that the two techniques may be equivalent. Further studies comparing the two techniques and using histopathology as a reference standard may confirm this impression.

In our study, native T1 map values were significantly higher in patients with higher liver histologic inflammation (PPA 2–3) compared to low inflammation stages (PPA

0–1), ($p=0.048$). The distinction between these groups has important clinical value, as histologic activity is essential for the therapeutic decision to discontinue or maintain immunosuppression [26]. These results support the idea that a simple, rapid, non-contrasted sequence may intervene in clinical decision-making and reduce the need for biopsy.

One of the main reasons for the use of cT1 is that in the presence of iron overload, T1 values can be influenced by the effects of iron, which can lead to an inaccurate interpretation [29]. However, in a population of pediatric AIH patients, an excellent positive correlation was observed between cT1 and native T1 relaxation times [42]. This relationship called into question the need for T1 iron correction in this patient population [42]. In this study, given the strength of the correlation and the fact that all 50 patients had normal liver T2* measurements, the authors concluded that T1 iron correction is probably not needed in pediatric AIH [42]. Again, there was no histologic correlation and significant systematic bias was reported between native T1 and cT1 measurements, so additional studies are needed before using uncorrected T1 map and cT1 interchangeably. In this sense, our study, performed in an adult population of AIH patients (none of them with iron accumulation according to the MRI R2* method), endorses the results of such a previous study carried out in a pediatric population, and this low burden of iron overload may (at least partially) explain why T1 mapping without iron correction may be so effective in the specific AIH population. Other alternatives to cT1 in patients affected by iron overload and steatosis are being currently studied (e.g., T1 mapping after hepatospecific contrast agent administration), with promising results [28, 43].

Taking into account the analysis of all T1 map measurement methods, it could be observed that the T1 map whole liver had a good performance in discriminating the fibrosis and inflammation groups. We identified cutoff points for T1 map to obtain the highest sensitivity and specificity according to the clinical objective desired: Advanced fibrosis 618.00 ms (MxSE) and 806.00 ms (MxSp); Significant fibrosis: 592.00 ms (MxSE) and 689.00 ms (MxSp) and Inflammatory activity 578.00 ms (MxSE) and 654.00 ms (MxSp).

Comparatively, T1 map values in other studies varied from 780 to 1100 for advanced and significant fibrosis. Conversely, the T1 map values for the different inflammation groups ranged from 780 to 1040 [10, 19, 40].

This study has several limitations. First, only a cross sectional design was used, with no follow-up of patients over time. New studies are needed to evaluate T1 mapping during clinical treatment prospectively. Second, T1 is a relaxation time dependent on field strength and biased by factors such as elevated iron concentration and steatosis. cT1 is a 'corrected' T1 relaxation time which is also adjusted for field strength differences, i.e., it corresponds to a T1

value that would have been measured in the presence of normal iron concentration on a Siemens Prisma 3 T scanner [44]; as our study was performed on a 1.5 T MRI machine, the results are only applicable to similar protocols. Thus, further studies on 3.0 T machines require validation using a specific protocol. Third, a relatively small number of AIH patients were included, but given the rarity of this disease, this sample is one of the largest in the literature. On the other hand, we have the advantage of a sample from the same population of patients, allowing for homogeneity: all patients undergone histological analysis, performed in the same center, by the same physician, allowing a reliable comparison of results with the gold standard method. We opted for an exclusive analysis by a single experienced pathologist to ensure homogeneity in the evaluation of the histological samples. Unfortunately, another limitation was the inability to perform analysis by two or more different pathologists because they were unavailable at our institution. At last, there was not a control group, but there were four F0 patients without inflammation, providing some idea of normal T1 values in the absence of any evidence of histopathologic change. Similarly, other studies in which the T1 map was evaluated in correlation with the biopsy did not have a control group [19, 40].

In conclusion, our findings suggest that a widely available MR sequence with an easy measurement technique such as uncorrected native T1 mapping has good diagnostic performance in the diagnosis of tissue fibrosis and inflammation in AIH. These methods have the potential to be valuable in monitoring inflammatory activity and fibrosis stage in a non-invasive manner. However, because of the difficulty in currently distinguishing fibrosis from hepatic inflammation using such a technique, future studies should address the issue, perhaps through the development of composite fibro-inflammatory histopathological and imaging scores with clinical validation, the combination of other outcome biomarkers (clinical or laboratory) with radiological ones, and, as part of this multiparametric MRI approach of the liver, the use of additional sequences such as T2 mapping.

Acknowledgements Not applicable.

Author contributions All authors contributed to the study conception and design. Material preparation and data collection were performed by Natalia e Ulysses. Analyses were performed by all authors. The first draft of the manuscript was written by Natália. All authors commented on previous versions of the manuscript. All authors read and approved the final manuscript.

Funding This study was financed in part by the Grupo Fleury (NP-312), Bayer (20884 / IIR-BR-2018–578), Coordenação de Aperfeiçoamento de Pessoal de Nível Superior—Brazil (CAPES)—Finance Code 001 and by the Conselho Nacional de Desenvolvimento Científico e Tecnológico—Brazil (CNPq)—Finance Code 150055/2019–6.

Data availability The datasets generated during the current study are available from the corresponding author on reasonable request.

Declarations

Conflict of interest The authors have no relevant conflict of interests to disclose.

Ethical approval All the procedures performed in studies involving human participants were in accordance with the ethical standards of the institutional and/or national research committee and with the 1964 Declaration of Helsinki and its later amendments or comparable ethical standards. This study obtained the approval of the Ethics Committee of the Federal University of São Paulo (approval number 97898718.6.3002.5474).

Informed consent Informed consent was obtained from all individual participants included in the study. This article does not contain any studies with animals performed by any of the authors.

References

- Ilyas JA, O'Mahony CA, Vierling JM (2011) Liver transplantation in autoimmune liver diseases. *Best Pract Res Clin Gastroenterol* 25:765–782. <https://doi.org/10.1016/j.bpg.2011.09.008>
- Manns MP, Czaja AJ, Gorham JD, Krawitt EL, Mieli-Vergani G, Vergani D, Vierling JM (2010) Diagnosis and management of autoimmune hepatitis. *Hepatology* 51:2193–2213. <https://doi.org/10.1002/hep.23584>
- Gomes NBN, Torres US, Ferraz MLCG, D'Ippolito G (2021) Autoimmune hepatitis in practice, from diagnosis to complications: what is the role of imaging? A clinicoradiological review. *Clin Imaging* 74:31–40. <https://doi.org/10.1016/j.clinimag.2020.12.032>
- Thomaides-Brears HB, Alkhouri N, Allende D, Harisinghani M, Nouredin M, Reau NS, French M, Pantoja C, Mouchti S, Cryer DRH (2022) Incidence of complications from percutaneous biopsy in chronic liver disease: a systematic review and meta-analysis. *Dig Dis Sci* 67:3366–3394. <https://doi.org/10.1007/s10620-021-07089-w>
- Bedossa P, Carrat F (2009) Liver biopsy: the best, not the gold standard. *J Hepatol* 50:1–3. <https://doi.org/10.1016/j.jhep.2008.10.014>
- Heneghan MA, Shumbayawonda E, Dennis A, Ahmed RZ, Rahim MN, Ney M, Smith L, Kelly M, Banerjee R, Culver EL (2022) Quantitative magnetic resonance imaging to aid clinical decision making in autoimmune hepatitis. *EClinicalMedicine* 46:101325. <https://doi.org/10.1016/j.eclinm.2022.101325>
- Bajre M, Moawad M, Shumbayawonda E, Carolan JE, Hart J, Culver E, Heneghan M (2022) LiverMultiScan as an alternative to liver biopsy to monitor autoimmune hepatitis in the National Health Service in England: an economic evaluation. *BMJ Open*. <https://doi.org/10.1136/bmjopen-2021-058999>
- Wang Q, Kesen S, Liljeroth M, Nilsson H, Zhao Y, Sparrelid E, Brismar TB (2022) Quantitative evaluation of liver function with gadoxetic acid enhanced MRI: Comparison among signal intensity-, T1-relaxometry-, and dynamic-hepatocyte-specific-contrast-enhanced MRI- derived parameters. *Scand J Gastroenterol* 57:705–712. <https://doi.org/10.1080/00365521.2022.2032321>
- Mesropyan N, Kupczyk P, Dold L, Weismüller TJ, Sprinkart AM, Mädler B, Pieper CC, Kuetting D, Strassburg CP, Attenberger

- U, Luetkens JA (2021) Non-invasive assessment of liver fibrosis in autoimmune hepatitis: diagnostic value of liver magnetic resonance parametric mapping including extracellular volume fraction. *Abdom Radiol* 46:2458–2466. <https://doi.org/10.1007/s00261-020-02822-x>
10. Arndtz K, Shumbayawonda E, Hodson J, Eddowes PJ, Dennis A, Thomaidis-Brears H, Mouchti S, Kelly MD, Banerjee R, Neubauer S, Hirschfield GM (2021) Multiparametric magnetic resonance imaging autoimmune hepatitis, and prediction of disease activity. *Hepatol Commun* 5:1009–1020. <https://doi.org/10.1002/hep4.1687>
 11. Janowski K, Shumbayawonda E, Cheng L, Langford C, Dennis A, Kelly M, Pronicki M, Grajkowska W, Wozniak M, Pawliszak P, Chelstowska S, Jurkiewicz E, Banerjee R, Socha P (2021) Quantitative multiparametric MRI as a non-invasive stratification tool in children and adolescents with autoimmune liver disease. *Sci Rep*. <https://doi.org/10.1038/s41598-021-94754-9>
 12. Janowski K, Shumbayawonda E, Dennis A, Kelly M, Bachtiar V, Debrot D, Langford C, Thomaidis-Brears H, Pronicki M, Grajkowska W, Wozniak M, Pawliszak P, Chelstowska S, Jurkiewicz E, Banerjee R, Socha P (2021) Multiparametric MRI as a noninvasive monitoring tool for children with autoimmune hepatitis. *J Pediatr Gastroenterol Nutr* 72:108–114. <https://doi.org/10.1097/MPG.0000000000002930>
 13. Pavlides M, Banerjee R, Sellwood J, Kelly CJ, Robson MD, Booth JC, Collier J, Neubauer S, Barnes E (2016) Multiparametric magnetic resonance imaging predicts clinical outcomes in patients with chronic liver disease. *J Hepatol* 64:308–315. <https://doi.org/10.1016/j.jhep.2015.10.009>
 14. Hoffman DH, Ayoola A, Nickel D, Han F, Chandarana H, Shanbhogue KP (2020) T1 mapping, T2 mapping and MR elastography of the liver for detection and staging of liver fibrosis. *Abdom Radiol* 45:692–700. <https://doi.org/10.1007/s00261-019-02382-9>
 15. Li Z, Sun J, Hu X, Huang N, Han G, Chen L, Zhou Y, Bai W, Yang X (2016) Assessment of liver fibrosis by variable flip angle T₁ mapping at 3.0T. *J Magn Reson Imaging* 43:698–703. <https://doi.org/10.1002/jmri.25030>
 16. Katsube T, Okada M, Kumano S, Hori M, Imaoka I, Ishii K, Kudo M, Kitagaki H, Murakami T (2011) Estimation of liver function using T1 mapping on Gd-EOB-DTPA-enhanced magnetic resonance imaging. *Invest Radiol* 46:277–283. <https://doi.org/10.1097/RLI.0b013e318200f67d>
 17. Breit HC, Block KT, Winkel DJ, Gehweiler JE, Henkel MJ, Weikert T, Stieltjes B, Boll DT, Heye TJ (2021) Heye, Evaluation of liver fibrosis and cirrhosis on the basis of quantitative T1 mapping: are acute inflammation, age and liver volume confounding factors? *Eur J Radiol*. <https://doi.org/10.1016/j.ejrad.2021.109789>
 18. Kim JW, Lee YS, Park YS, Kim BH, Lee SY, Yeon JE, Lee CH (2020) Multiparametric MR Index for the diagnosis of non-alcoholic steatohepatitis in patients with non-alcoholic fatty liver disease. *Sci Rep*. <https://doi.org/10.1038/s41598-020-59601-3>
 19. von Ulmenstein S, Bogdanovic S, Honcharova-Biletska H, Blümel S, Deibel AR, Segna D, Jüngst C, Weber A, Kuntzen T, Gubler C, Reiner CS (2022) Assessment of hepatic fibrosis and inflammation with look-locker T1 mapping and magnetic resonance elastography with histopathology as reference standard. *Abdom Radiol* 47:3746–3757
 20. Torres US, D'ippolito G (2021) Multiparametric magnetic resonance imaging of the liver: bridging the gap between theory and practice—a bridge too far? *Radiol Bras* 54:5–6. <https://doi.org/10.1590/0100-3984.2021.54.5e1>
 21. Hennes EM, Zeniya M, Czaja AJ, Pares A, Dalekos GN, Krawitt EL, Bittencourt PL, Porta G, Boberg KM, Hofer H, Bianchi FB, Shibata M, Schramm C, Eisenmann de Torres B, Galle PR, McFarlane I, Dienes H-P, Lohse AW (2008) Simplified criteria for the diagnosis of autoimmune hepatitis. *Hepatology* 48:169–176. <https://doi.org/10.1002/hep.22322>
 22. Rockey DC, Caldwell SH, Goodman ZD, Nelson RC, Smith AD (2009) Liver biopsy. *Hepatology* 49:1017–1044. <https://doi.org/10.1002/hep.22742>
 23. Group TFMCS, Bedossa P (1994) Intraobserver and interobserver variations in liver biopsy interpretation in patients with chronic hepatitis C. *Hepatology* 20 15–20 <https://doi.org/10.1002/hep.1840200104>
 24. Ishak K, Baptista A, Bianchi L, Callea F, De Groote J, Gudat F, Denk H, Desmet V, Korb G, MacSween RNM, Phillips MJ, Portmann BG, Poulsen H, Scheuer PJ, Schmid M, Thaler H (1995) Histological grading and staging of chronic hepatitis. *J Hepatol* 22:696–699. [https://doi.org/10.1016/0168-8278\(95\)80226-6](https://doi.org/10.1016/0168-8278(95)80226-6)
 25. Desmet VJ, Gerber M, Hoofnagle JH, Manns M, SCHEUER JH (1994) Scheuer, classification of chronic hepatitis: diagnosis, grading and staging. *Hepatology* 19:1513–1520. <https://doi.org/10.1002/hep.1840190629>
 26. Harrison L, Gleeson D (2019) Stopping immunosuppressive treatment in autoimmune hepatitis (AIH): is it justified (and in whom and when)? *Liver Int* 39:610–620. <https://doi.org/10.1111/liv.14051>
 27. Hernando D, Zhao R, Yuan Q, Aliyari Ghasabeh M, Ruschke S, Miao X, Karampinos DC, Mao L, Harris DT, Mattison RJ, Jeng MR, Pedrosa I, Kamel IR, Vasanawala S, Yokoo T, Reeder SB (2022) Reeder, multicenter reproducibility of liver iron quantification with 1.5-T and 3.0-T MRI. *Radiology* 306:e213256. <https://doi.org/10.1148/radiol.213256>
 28. Yoon JH, Lee JM, Paek M, Han JK, Choi BI (2016) Quantitative assessment of hepatic function: modified look-locker inversion recovery (MOLLI) sequence for T1 mapping on Gd-EOB-DTPA-enhanced liver MR imaging. *Eur Radiol* 26:1775–1782. <https://doi.org/10.1007/s00330-015-3994-7>
 29. Banerjee R, Pavlides M, Tunnicliffe EM, Piechnik SK, Sarania N, Philips R, Collier JD, Booth JC, Schneider JE, Wang LM, Delaney DW, Fleming KA, Robson MD, Barnes E, Neubauer S (2014) Multiparametric magnetic resonance for the non-invasive diagnosis of liver disease. *J Hepatol* 60:69–77. <https://doi.org/10.1016/j.jhep.2013.09.002>
 30. Mahalingam N, Trout AT, Gandhi DB, Sahay RD, Singh R, Miethke AG, Dillman JR (2022) Associations between MRI T1 mapping, liver stiffness, quantitative MRCP, and laboratory biomarkers in children and young adults with autoimmune liver disease. *Abdom Radiol* 47:672–683. <https://doi.org/10.1007/s00261-021-03378-0>
 31. Catucci D, Obmann VC, Berzigotti A, Gräni C, Guensch DP, Fischer K, Ebner L, Heverhagen JT, Christe A, Huber AT (2021) Noninvasive assessment of clinically significant portal hypertension using ΔT_1 of the liver and spleen and ECV of the spleen on routine Gd-EOB-DTPA liver MRI. *Eur J Radiol*. <https://doi.org/10.1016/j.ejrad.2021.109958>
 32. Georgoff P, Thomasson D, Louie A, Fleischman E, Dutcher L, Mani H, Kottlilil S, Morse C, Dodd L, Kleiner D, Hadigan C (2012) Hydrogen-1 MR spectroscopy for measurement and diagnosis of hepatic steatosis. *Am J Roentgenol* 199:2–7. <https://doi.org/10.2214/AJR.11.7384>
 33. Longo R, Pollesello P, Ricci C, Masutti F, Kvam BJ, Bercich L, Croce LS, Grigolato P, Paoletti S, De Bernard B, Tiribelli C, Dalla Palma L (1995) Proton MR spectroscopy in quantitative in vivo determination of fat content in human liver steatosis. *J Magn Reson Imaging* 5:281–285. <https://doi.org/10.1002/jmri.1880050311>

34. Reeder SB, Yokoo T, França M, Hernando D, Alberich-Bayarri A, Alústiza JM, Gandon Y, Henninger B, Hillenbrand C, Jhaveri K, Karçaaltıncaba M, Kühn JP, Mojtahed A, Serai SD, Ward R, Wood JC, Yamamura J, Martí-Bonmatí L (2023) Quantification of liver iron overload with MRI: review and guidelines from the ESGAR and SAR. *Radiology*. <https://doi.org/10.1148/radiol.221856>
35. Starekova J, Hernando D, Pickhardt PJ, Reeder SB (2021) Quantification of liver fat content with CT and MRI: state of the art. *Radiology* 301:250–262. <https://doi.org/10.1148/radiol.2021204288>
36. Henninger B, Alustiza J, Garbowski M, Gandon Y (2020) Practical guide to quantification of hepatic iron with MRI. *Eur Radiol* 30:383–393. <https://doi.org/10.1007/s00330-019-06380-9>
37. Czaja AJ (2014) Hepatic inflammation and progressive liver fibrosis in chronic liver disease. *World J Gastroenterol* 20:2515–2532. <https://doi.org/10.3748/wjg.v20.i10.2515>
38. Obmann VC, Catucci D, Berzigotti A, Gräni C, Ebner L, Heverhagen JT, Christe A, Huber AT (2022) T1 reduction rate with Gd-EOB-DTPA determines liver function on both 1.5 T and 3 T MRI. *Sci Rep*. <https://doi.org/10.1038/s41598-022-08659-2>
39. Pavlides M, Banerjee R, Tunnicliffe EM, Kelly C, Collier J, Wang LM, Fleming KA, Cobbold JF, Robson MD, Neubauer S, Barnes E (2017) Multiparametric magnetic resonance imaging for the assessment of non-alcoholic fatty liver disease severity. *Liver Int* 37:1065–1073. <https://doi.org/10.1111/liv.13284>
40. Trout AT, Taylor AE, Kasten JL, Castro-Rojas C, Mahalingam N, Miethke AG, Dillman JR (2023) Corrected T1 mapping in children and young adults with autoimmune liver disease: correlation with histology. *AJR Am J Roentgenol* 220:901–902. <https://doi.org/10.2214/AJR.22.28765>
41. Thomaidis-Brears HB, Lepe R, Banerjee R, Duncker C (2020) Multiparametric MR mapping in clinical decision-making for diffuse liver disease. *Abdom Radiol* 45:3507–3522. <https://doi.org/10.1007/s00261-020-02684-3>
42. Dillman JR, Serai SD, Miethke AG, Singh R, Tkach JA, Trout AT (2020) Comparison of liver T1 relaxation times without and with iron correction in pediatric autoimmune liver disease. *Pediatr Radiol* 50:935–942. <https://doi.org/10.1007/s00247-020-04663-8>
43. Unal E, Idilman IS, Karçaaltıncaba M (2017) Multiparametric or practical quantitative liver MRI: towards millisecond, fat fraction, kilopascal and function era. *Expert Rev Gastroenterol Hepatol* 11:167–182. <https://doi.org/10.1080/17474124.2017.1271710>
44. Bachtiar V, Kelly MD, Wilman HR, Jacobs J, Newbould R, Kelly CJ, Gyngell ML, Groves KE, McKay A, Herlihy AH, Fernandes CC, Halberstadt M, Maguire M, Jayaratne N, Linden S, Neubauer S, Banerjee R (2019) Repeatability and reproducibility of multiparametric magnetic resonance imaging of the liver. *PLoS ONE* 14:e0214921. <https://doi.org/10.1371/journal.pone.0214921>

Publisher's Note Springer Nature remains neutral with regard to jurisdictional claims in published maps and institutional affiliations.

Springer Nature or its licensor (e.g. a society or other partner) holds exclusive rights to this article under a publishing agreement with the author(s) or other rightsholder(s); author self-archiving of the accepted manuscript version of this article is solely governed by the terms of such publishing agreement and applicable law.